PRESSURE DISTRIBUTION AROUND A SINGLE BUBBLE MOVING IN A FLUIDIZED BED

V. G. Kul'bachnyi and K. E. Makhorin

UDC 532.546

Results are presented on the pressure distribution within a bubble and around it, the bubble being in a fluidized bed.

The structure of a fluidized bed changes appreciably when gas bubbles appear. The dynamic parameters are determined in the main by the hydrodynamics of the fluidization, and the result is transient-state motion of the solid phase and gas, together with pressure pulsations and local variations in the density.

The stability of the gas bubbles (discrete phase) and the ejection of material when they break up at the surface indicate that the cavity within the bubble is at a pressure higher than that of the surrounding medium (continuous phase).

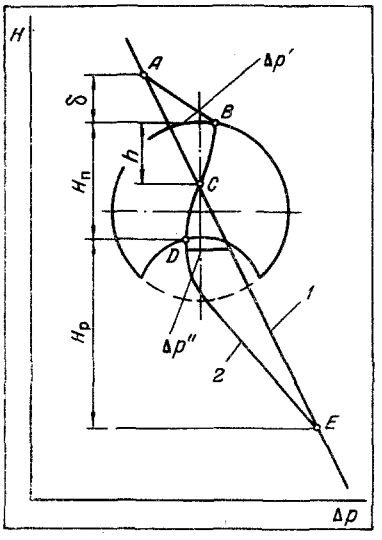

Fig. 1

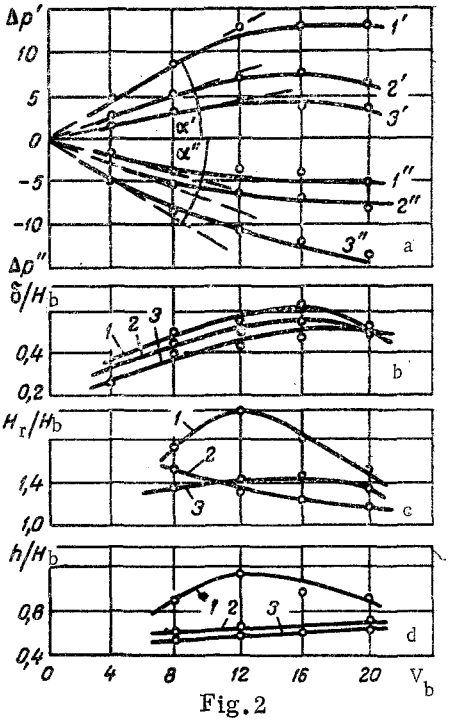

Fig. 2

Fig. 1. Pressure distribution in a bed with: 1) uniform fluidization; 2) a gas bubble within it.

Fig. 2. Effects of bubble size on the pressure distribution in a fluidized bed of graphite particles: 1) 0.106 mm; 2) 0.172 mm; 3) 0.3 mm; a) $\Delta p'$ and $\Delta p''$ (mm water) as functions of bubble volume V_b (cm^3); b-d) δ/H_b, H_r/H_b, and h/H_b as functions of V_b; α is the slope of the tangent.

Institute of Gas, Academy of Sciences of the Ukrainian SSR. Translated from Inzhenerno-Fizicheskii Zhurnal, Vol. 21, No. 6, pp. 998-1004, December, 1971. Original article submitted February 6, 1971.

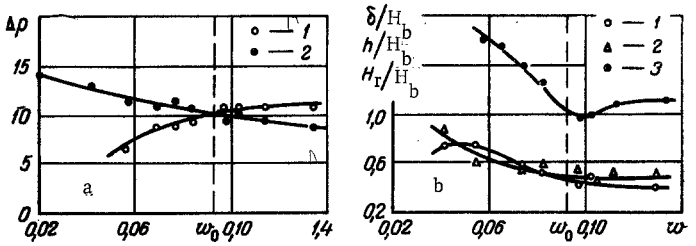

Fig. 3. Effects of speed w (m/sec) of fluidizing agent on the distribution of the pressure Δp (mm water) in and around the bubble for particles with d_e = 0.254 mm and V_b = 16 cm^3; a) $\Delta p''$ (curve 1) and $\Delta p'$ (curve 2) as functions of w; b) δ/H_b (curve 1), h/H_b (curve 2), and H_r/H_b (curve 3) as functions of w.

Experimental results [1-3] and theoretical studies [4-7] show that only the upper part of the bubble cavity is under excess pressure, whereas the lower part shows reduced pressure, i.e., the leading edge has a positive pressure gradient while the trailing one has a negative one.

These different signs for the pressure gradient along the vertical axis go with the gas-permeable surface to facilitate gas transfer between the discrete and continuous phases.

The rate of gas flow through the cavity determines the type of motion of the discrete phase [4, 8] and is itself dependent on the pressure gradient and the porosity of the surrounding medium.

Here we report tests on the pressure around and within a bubble.

The tests were done on a laboratory system: in a column 75 mm diameter we used particles of conducting material (graphite) with a narrow grain-size distribution and an equivalent diameter of 0.106, 0.172, 0.254, or 0.3 mm. Air was the fluidizing agent. The experiments were done under normal conditions. The height of the fluidized layer was equal to the column diameter. Into the fluidized layer we injected an additional volume of air, which was used to produce a single bubble. We observed the motion of the bubble with a probe, which consisted of two graphite electrodes 1 mm in diameter and a pressure detector in the form of a tube 3 mm in diameter. The electrode lengths and distance between them were 3 mm. The electrodes were connected in the circuit of a type M001 galvanometer. The pressure detector was connected to an optical pressure transducer. The galvanometer and the pressure transducer were connected to an N700 oscillograph. The passage of the gas bubble past the point of observation was accompanied by interruption of the galvanometer circuit and change in the pressure; the readings of the galvanometer and pressure transducer were recorded on photographic paper.

The results from the oscillograms showed that this was a sound method of performing the experiments and provided some quantitative relationships.

Figure 1 shows the pressure distribution in height for the main body of the bed with uniform fluidization (line 1) and with the single gas bubble present (curve 2). The upper part of the bubble of height h and a certain region above the bubble of extent δ were under excess pressure with relation to the surrounding medium, while the lower part of the bubble of height $(H_b - h)$ and a zone beneath it of depth H_r were under reduced pressure. Part b of the zone represented a sheath of particles with a porosity equal to that of the unfluidized bed.

There was a small pressure difference over the height of the bubble; in the leading part of the bubble (point B) the pressure was higher than that in the trailing part (point D). This type of pressure distribution in a bubble has been reported before [2].

The vertical pressure gradient occurs because curve ABCDE reflects the change in the static pressure difference, whose distribution in the bubble cavity is dependent on the gas speed in the bubble. The motion of the bubble is accompanied by a transverse flow through the cavity and a circulatory motion within it [4]. At point D, these flows add up, and the speed of the overall flow attains values such as to set up a dynamic pressure head, which results in reduced static pressure at this point. In the part CB there is a dispersal of the jet, the gas speed falls, the static pressure increases, and a point B is one of maximal pressure.

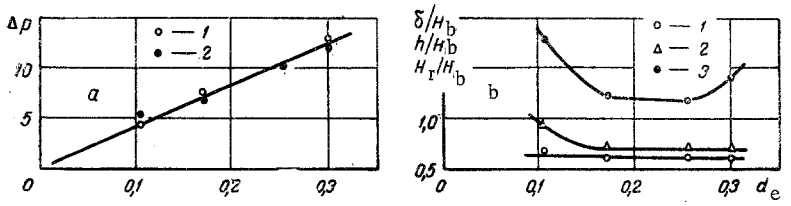

Fig. 4. Effects of d_e (mm) on Δp (mm water) in and around bubble for $w = w_0$ and $V_b = 16$ cm^3: a) $\Delta p'$ (curve 1) and $\Delta p''$ (curve 2); b) δ/H_b (curve 1), h/H_b (curve 2), and H_r/H_b (curve 3) as functions of w.

The excess pressure $\Delta p'$ at point B relative to the surrounding medium is determined by the leakage of gas from the bubble cavity, while the negative pressure $\Delta p''$ at point D characterizes the influx of gas into the bubble. The zone of excess pressure δ above the bubble and the zone of rarefaction H_r behind it reflect the hydrodynamic state of the layer around the bubble and the rate of transfer of gas between the discrete and continuous phases, as does the proportion h of the height under excess pressure. The values of $\Delta p'$, $\Delta p''$, δ, H_r, and h are dependent on the bubble volume, the speed of the fluidizing flow, and the particle size.

Figure 2 shows how $\Delta p'$ and $\Delta p''$ are dependent on the initial volume V_b of the bubble for the three graphite fractions 1-3 having equivalent diameters of 0.106, 0.172, and 0.3 mm.

We see that $\Delta p'$ and $\Delta p''$ increase linearly with the bubble volume in the range $D/D_b \geq 2.53$; any subsequent increase in V_b leads to less pronounced increase in $\Delta p''$ and an appreciable reduction in $\Delta p'$ for $D/D_b \geq 2.28$, where D and D_b are the diameters of the tube and bubble. D_b was determined from the previously derived relationship $V_b = 0.453\, D_b^3$.

Tangents drawn to the $\Delta p'$ and $\Delta p''$ curves through the origin differ in slope ($\alpha' = \alpha''$) for corresponding particle sizes, which confirms that $|\Delta p'| = |\Delta p''|$ as reported in [2, 3].

Parts b-d of Fig. 2 give the behavior of δ/H_b, H_r/H_b, h/H_b in response to the initial size of the bubble; a characteristic feature in each case is that the perturbed region around the bubble is larger when the particles are smaller, which is due to change in the viscosity characteristics of the bed. The effective viscosity of the fluidized bed increases with the particle size [9], which affects the fluidity and hence the deformation of a layer over a surrounding region.

Figure 2b shows that δ/H_b increases with V_b within certain limits; the excess-pressure zone above the bubble grows with the bubble size on account of the increased pressure in the upper part of the bubble; δ increases with $\Delta p'$ for the constant gas flow from the bubble into a layer of unchanged porosity. The relation between $\Delta p'$ and δ may be described to a first approximation by an equation for the flow of liquid from a spherical source [10].

Figure 2c shows H_r/H_b as a function of V_b, where curve 1 corresponds to an equivalent particle size of 0.106 mm; for $D/D_b = 2.53$ there is a peak, and the depth of the rarefaction zone in this case is more than twice the height of the bubble. Further, H_r is only about 1.4 H_b for particles of equivalent diameter 0.172 or 0.3 mm for the same D/D_b. Increase in V_b reduces H_r/H_b for particles of equivalent diameter 0.172 mm throughout the range employed, whereas for particles of size 0.3 mm there was an increase in this quantity only for $D/D_b \geq 2.28$, this being followed by a fall.

Figure 2d shows h/H_b as a function of H_b; there is a peak in this quantity, with $h > H_b$ for the 0.106 mm particles (curve 1) for $D/D_b = 2.53$; clearly, under these conditions one gets a bubble cavity similar in shape to a segment of a sphere. The gas flow through the bottom of the bubble entrains particles and tends to fill the bottom of the bubble to a greater extent than when large particles are used. Then H_b is naturally reduced and h exceeds it. With particles of 0.172 or 0.3 mm, h/H_b increases with V_b, and the increase in h is linear in the range of V_b of 8-20 cm^3.

There is an appreciable change in the dependence of $\Delta p'$, $\Delta p''$, δ/H_b, h/H_b, H_r/H_b on V_b for certain D/D_b on account of the apparatus size; the nearness of the walls affects the bubble motion for $D/D_b \leq 3.0$ [4].

Figure 3a shows how $\Delta p'$ and $\Delta p''$ are dependent on w; $\Delta p'$ decreases as w increases, while $\Delta p''$ increases.

We found that the gas bubbles can exist also in an immobile layer; as the bubble rises, its volume decreases, and δ also diminishes as w increases (curve 1 of Fig. 3b), which results in a reduction in the hydrodynamic resistance. The rate of gas leakage from the bubble increases, and the pressure in the leading part falls, and hence the pressure throughout the cavity, which means an increase in the rarefaction $\Delta p''$ in the lower part.

Curve 2 of Fig. 3b reflects the dependence of h/H_b on w; before fluidization starts, there is a sharp fall in h/H_b, whereas there is only a minor change for $w > w_0$. The fall in h as w increases occurs on account of the increased pressure drop in the continuous phase, which means that part of the gas flow traveling with the bubble enters into the cavity, since the hydrodynamic resistance in that part is less, which in turn tends to equalize the pressures in the lower and upper parts of the bubble cavity.

Curve 3 of Fig. 3b reflects the variation in H_r with w; in an immobile layer, H_r/H_b falls markedly, and it reaches its minimal value for $w = 1.15\, w_0$. Any further increase in the flow speed causes a tendency to a constant value $H_r \simeq 1.1\, H_b$.

Figure 4a reveals a direct proportionality in the effect of the particle size on $\Delta p'$ and $\Delta p''$; increase in d_e results in increases in the latter two quantities. The observed points for $\Delta p'$ and $\Delta p''$ fit satisfactorily to a single straight line, which confirms $|\Delta p'| = |\Delta p''|$ for $w = w_0$ [2].

The size of the channels between particles increases with the particle size itself, and this reduces the hydrodynamic resistance, which should cause a reduction in the pressure in the upper part of the bubble; however, increase in $\Delta p'$ goes in hand with an increase in $\Delta p''$, the latter being due to the properties of the surrounding medium, i.e., the cross section of the pore channels increases with the grain size, the hydrodynamic resistance falls, and hence one gets a more rapid equalization of the pressure between the surrounding medium and the lower end of the bubble.

There is thus a continuous equilibrium between $\Delta p'$ and $\Delta p''$, while the absolute values of these are determined by the properties of the surrounding medium.

Figure 4b shows that the fall in δ/H_b as d_e increases is only slight, and to a certain approximation we may assume that δ is independent of the particle size; however, Fig. 2b shows that any increase in V_b, and thus in $\Delta p'$ (Fig. 2a), will result in an increase in δ/H_b. Figure 4a shows that $\Delta p'$ increases with d_e, which in turn should lead to increase in δ/H_b.

This behavior of δ/H_b cannot be explained on the basis of concepts concerning the viscous stresses in the layer acting as a continuous medium.

The fall in the pressure gradient between the bubble and the surrounding medium is governed not only by the effective viscosity of the layer, which characterizes the layer as a continuous medium, but also by the porosity, i.e., by the size of the pore channels. The pressure may be equalized as a result of flow of the continuous phase as a liquid, i.e., as a result of simultaneous motion of the particles of the gas as well as of the motion of the gas alone between the particles.

The first effect is determined by the viscosity of the layer, and the second by the dimensions of the pore channels in the fluidized bed; the two effects occur together, and the predominance of one or the other is dependent on the properties of the system, of which the main one is the particle size. The viscosity increases with the particle diameter, and the tendency of the medium to flow is reduced, with the result that there is less tendency for pressure equalization by motion of the continuous phase (particles and gas). The channel diameter also increases with the particle diameters, and the pressure equalization will therefore tend to occur by flow of gas through the channels when the particles are large.

We therefore consider that the picture of the gas flow above the bubble is as follows. If the particles are small, the escape of gas from the bubble and dispersal through the layer encounters a hydrodynamic resistance greater than that in the layer of large particles, which results in a difference in the gas leakage rates and hence in the size of the excess-pressure zone above the bubble. In the first case, the medium is more fluid, and the pressure gradient is reduced above the sheath of immobile particles mainly as a result of motion of the continuous phase. If the particles are large, the effect occurs by motion of the gas in the pore channels.

We find that h/H_b tends to decrease as the particle size increases in the range $d_e \leq 0.165$ mm (curve 2 of Fig. 4b); further change in d_e has little effect on this quantity.

Curve 3 of Fig. 4b reflects the variation in H_r with d_e; in the range 0.165-0.265 mm there is only a slight change in H_r/H_b, but any further increase in d_e causes an appreciable rise in the latter. The relationship may be divided crudely into three regions: in the first (d_e < 0.165 mm) the viscosity increases with the particle size, so the moving bubble remains turbulent (entrained jet), and this turbulence dies away only slowly on account of the inertial forces of the particles in a medium of low viscosity. In the second region (d_e = 0.165-0.265 mm) the increase in viscous stresses is balanced by increase in the size of the channels between grains, and there is increased influx of gas from the continuous phase, with a fall in the rate of reduction in the rarefaction zone. In the third region (d_e > 0.265 mm) the sizes of the channels between the particles become sufficient for the pressure equalization to occur mainly by flow in the channels, while the thickness of the rarefaction zone increases on account of the increased influx of gas into the bubble cavity from a large volume of the layer.

NOTATION

$\Delta p'$ is the excess pressure at the front of the bubble;
$\Delta p''$ is the rarefaction at the rear of the bubble;
δ is the height of the excess pressure region over the bubble;
H_b is the height of the bubble;
H_r is the height of the region of rarefaction behind the bubble;
h is the part of the bubble cavity under excess pressure;
V_b is the initial volume of the bubble;
w is the velocity of the fluidizing agent;
w_0 is the velocity of the onset of fluidization;
d_e is the equivalent diameter of a particle;
D is the diameter of the apparatus;
D_b is the bubble diameter.

LITERATURE CITED

1. P. F. Wace and S. J. Burnett, Trans. Inst. Chem. Eng., 39, No. 3 168-174 (1961).
2. H. Reuter, Chem.-Ing. Techn., 35, No. 2, 98-103 (1963).
3. H. Reuter, Chem.-Ing. Techn., 35, No. 3, 219-224 (1963).
4. J. F. Davidson and D. Harrison, Fluidization of Solid Particles [Russian translation], Khimiya (1965).
5. R. Collins, Chem. Eng. Sci., 20, No. 8, 747-755 (1965).
6. R. Jackson, Trans. Inst. Chem. Eng., 41, No. 1, 22-28 (1963).
7. J. D. Murray, J. Fluid Mech., 22, 57-80 (1965).
8. L. Davies and J. F. Richardson, Trans. Inst. Chem. Eng., 44, No. 8, 293-305 (1966).
9. F. Z. Grek and V. N. Kisel'nikov, Zh. Prikl. Khim., 35, No. 10, 22-35 (1962).
10. V. I. Aravin and S. N. Numerov, Theory of the Motion of Liquids and Gases in a Rigid Porous Medium [in Russian], GITTL (1953).